Struct Multidisc Optim (2012) 45:223–233
DOI 10.1007/s00158-011-0680-5

RESEARCH PAPER

An isogeometrical approach to structural topology optimization by optimality criteria

Behrooz Hassani · Mostafa Khanzadi · S. Mehdi Tavakkoli

Received: 11 February 2010 / Revised: 7 June 2011 / Accepted: 10 June 2011 / Published online: 23 July 2011

Abstract The Isogeometric Analysis (IA) method is applied for structural topology optimization instead of finite elements. For this purpose, a control point based Solid Isotropic Material with Penalization (SIMP) method is employed and the material density is considered as a continuous function throughout the design domain and approximated by the Non-Uniform Rational B-Spline (NURBS) basis functions. To prevent the formation of layouts with porous media, a penalization technique similar to the SIMP method is used. For optimization an optimality criteria is derived and implemented. A few examples are presented to demonstrate the performance of the method. It is shown that, dissimilar to the element based SIMP topology optimization, the resulted layouts by this method are independent of the number of the discretizing control points and checkerboard free.

Keywords Structural topology optimization · Isogeometric analysis · SIMP method

1 Introduction

Structural topology optimization methods have made remarkable progress in recent years. This kind of optimization is employed mainly to specify the optimum number and location of holes in the configuration of the structure which is usually followed by shape optimization in order to find optimum boundaries. Topology optimization has received enormous attention since the introduction of the homogenization approach to topology optimization by Bendsøe and Kikuchi (1988) but its origin goes back to the minimum weight structures of Michell (1904).

To solve the topology optimization problem any nonlinear mathematical programming method may be used. Despite being robust, due to the large number of design variables, application of these methods to the topology optimization problems is relatively more costly and time consuming. The Optimality Criteria (OC) methods are proved to be amongst the most effective to solve the topology optimization problems (Rozvany 1989) and hence are used in this research work. However, several different methods such as the approximation methods (Schmit and Farsi 1974; Schmit and Miura 1976; Vanderplaats and Salajegheh 1989), CONLIN (Fleury 1989) and the method of moving asymptotes (MMA) (Svanberg 1987), even more heuristic methods such as genetic algorithm (Kane and Schoenauer 1996; Fanjoy and Crossley 2000; Jakiela et al. 2000) and Ant colony (Kaveh et al. 2008) are employed for this purpose. Also, less mathematically rigorous methods such as the evolutionary structural optimization method (ESO) (Xie and Steven 1993) can be named. Recently several different approaches are devised that uses the level set methods (Sethian and Wiegmann 2000; Wang et al. 2003; Allaire et al. 2004; Belytschko et al. 2003). A recent review of topology optimization methods was offered by Rozvany (2010).

The methods mentioned above for structural topology optimization are mostly element based, where the material density function is a constant within each finite element.

B. Hassani (✉)
Department of Civil Engineering, Shahrood University of Technology, Shahrood, 36155, Iran
e-mail: b_hassani@iust.ac.ir

M. Khanzadi · S. M. Tavakkoli
Department of Civil Engineering, Iran University of Science and Technology, Narmak, Tehran, Iran

The nodal based methods have more recently introduced by Belytschko et al. (2003) and have been used in topology optimization together with mesh free methods (Zhou and Zou 2008). In these approaches the material densities are determined at the discretization nodes or points. The method presented in this article falls within the category of nodal based methods which uses control points instead of nodal points and employs the recently developed IA approach.

IA is a relatively new method proposed and developed by Hughes and his co-workers in recent years (Hughes et al. 2005; Bazilevs et al. 2006a, b, 2007; Cottrell et al. 2006). This method is a logical extension and generalization of the classical finite element method and has many features in common with it. However, it is more geometrically based and takes inspiration from Computer Aided Geometry Design (CAGD). A primary goal of IA is to be geometrically precise no matter how coarse the discretization beside simplification of mesh refinement by eliminating the need for communication with the CAD geometry once the initial model is constructed. The main idea of the method is to use the same basis functions which are employed for geometry description for approximation and interpolation of the unknown field variables as well. Due to some interesting properties of B-splines and NURBS, they are perfect candidates for this purpose.

In structural topology design the optimum distribution of a given material, mostly isotropic, in a defined domain is searched (Hassani and Hinton 1999; Bendsøe and Sigmund 2003). The material assigned to each point of the design domain can be specified by a material distribution function. Different from element based topology optimization problems where the material distribution function is a element-wise step function, in this paper the material distribution function is approximated over the whole domain by using NURBS and is restricted to be within the zero (for empty areas or voids) and one (for solid areas) interval. Also, similar to the SIMP method (Zhou and Rozvany 1991; Rozvany et al. 1992), to suppress formation of undesirable porous media inside the optimal layout, a penalty exponent is implemented. In other words, the difference between the proposed method and the conventional SIMP method, where an artificial material model with constant values of the material properties within the finite elements is used, is that the material density is considered as an imaginary (hyper-)surface over the domain of the problem.

The outline of this paper is as follows. In Section 2, the IA method for plane stress problems is briefly explained. Section 3 is devoted to the concise definition of topology optimization problem. Modeling of the material density distribution and derivation of the optimality criteria is the subject of Section 4. In Section 5 a few examples are presented to demonstrate the performance of the method. The results are discussed in the last section.

2 Isogeometrical analysis

By recent developments in the CAGD technology, the geometrical definition and generation of complex surfaces and objects have become achievable (Piegl and Tiller 1997). For this purpose, Splines and some modified versions of them, i.e. NURBS and T-Splines, are commonly employed. The main idea in the IA method is that any component of a field variable which satisfies a governing partial differential equation, i.e. the solution, is imagined as a (hyper-)surface that can be constructed by the proper versions of splines (Hassani et al. 2009a, b). For example, in displacement method for elasticity problems, each of the components of the displacement vector is considered as a surface which can be constructed by NURBS and the defining parameters of these surfaces are sought. The criteria for finding these parameters can be obtained by minimizing a total potential energy functional or equivalently by implementation of the virtual work principle.

The IA method has some features in common with other numerical methods such as finite elements and meshfree methods. Discretization of the domain of interest is performed by using the control points of splines instead of, for instance, using the finite element meshes, finite difference grids, or collection of points in the meshfree methods. Also, the basis functions of these splines are used both for approximation of the unknown variables as well as for interpolation.

The procedure of the IA for elasticity problems is comprised of the following steps. First, the geometry of the domain of interest is constructed by using the NURBS technology. Depending on the complexity of the geometry and topology of the problem, multiple NURBS patches can be used in this stage. These patches may be thought of as kind of macro elements in the finite element method and can be assembled in the same fashion (Hughes et al. 2005). In the next step, borrowing the ideas from isoparametric finite elements, the geometry as well as the displacement components are approximated by making use of the NURBS basis functions. Then, following a standard procedure like the weighted residuals or the variational methods, or similarly using the principle of virtual work, the approximated quantities are substituted into the obtained relations. This will result in a system of linear equations to be solved. One should note that following this procedure the control variables are evaluated and to obtain the displacements at certain points a kind of post processing is required. A brief introduction to the construction of NURBS surfaces followed by derivation of IA formulation

for plane elasticity problems are the subjects of the next two subsections.

2.1 Surface and volume definition by NURBS

A NURBS surface is parametrically constructed as (Piegl and Tiller 1997)

$$S(r,s)=\sum_{i=0}^{n_1}\sum_{j=0}^{n_2}\frac{N_{i,p_1}(r)\;N_{j,p_2}(s)\;\omega_{i,j}}{\sum_{k=0}^{n_1}\sum_{l=0}^{n_2}N_{k,p_1}(r)\,N_{l,p_2}(s)\;\omega_{k,l}}P_{i,j} \tag{1}$$

where $P_{i,j}$ are $(n_1+1)\times(n_2+1)$ control points, $\omega_{i,j}$ are the associated weights, and $N_{i,p_1}(r)$ and $N_{j,p_2}(s)$ are the normalized B-splines basis functions of degree p_1 and p_2, respectively. The i-th B-spline basis function of degree p_1, denoted by $N_{i,p_1}(r)$, is defined recursively as:

$$N_{i,0}(r)=\begin{cases}1 & \text{if}\quad r_i\le r\le r_{i+1}\\ 0 & \text{otherwise}\end{cases} \tag{2}$$

$$N_{i,p_1}=\frac{r-r_i}{r_{i+p_1}-r_i}N_{i,p_1-1}(r)+\frac{r_{i+p_1+1}-r}{r_{i+p_1+1}-r_{i+1}}N_{i+1,p_1-1}(r)$$

where $\mathbf{r}=\{r_0,r_1,\ldots,r_{m_1}\}$ is the knot vector and r_i are a non-decreasing sequence of real numbers, which are called knots. The knot vector $\mathbf{s}=\{s_0,s_1,\ldots,s_{m_2}\}$ is employed to define the $N_{j,p_2}(s)$ basis functions for other direction. The interval $[r_0,r_{m_1}]\times[s_0,s_{m_2}]$ forms a Patch (Hughes et al. 2005). A knot vector, for instance in r direction, is called open if the first and last knots have a multiplicity of p_1+1. In this case, the number of knots is equal to $m_1=n_1+p_1+1$. Also, the interval $[r_i,\,r_{i+1})$ is called a knot span where at most p_1+1 of the basis functions $N_{i,p_1}(r)$ are non-zero which are $N_{i-p_1,p_1}(r),\ldots,N_{i,p_1}(r)$. For more details Piegl and Tiller (1997) can be consulted.

2.2 Numerical formulation for plane elasticity problems

In the isogeometric analysis method, the domain of problem might be divided into subdomains or patches so that B-spline or NURBS parametric space is local to these patches. A patch is like an element in the finite element method and the approximation of unknown function can be written over a patch. Therefore, the global coefficient matrix, which is similar to the stiffness matrix in elasticity problems, can be constructed by employing the conventional assembling which is used in the finite element method.

By using the NURBS basis functions for a patch p, the approximated displacement functions $\mathbf{u}^p=[u,\,v]$ can be written as

$$\mathbf{u}^p(r,s)=\sum_{i=0}^{n_1}\sum_{j=0}^{n_2}R_{i,j}(r,s)\,\mathbf{u}^p_{i,j} \tag{3}$$

where $R_{i,j}(r,s)$ is the rational term in (1). It should be noted that the geometry is also approximated by B-spline basis functions as

$$\mathbf{x}^p(r,s)=\sum_{i=0}^{n_1}\sum_{j=0}^{n_2}R_{i,j}(r,s)\,\mathbf{x}^p_{i,j}. \tag{4}$$

By using the local support property of NURBS basis functions, the above relation can be summarized as it follows in any given $(r,s)\in[r_i,r_{i+1})\times[s_j,s_{j+1})$.

$$\mathbf{u}^p(r,s)=\sum_{e=i-p_1}^{i}\sum_{f=j-p_2}^{j}R_{e,f}(r,s)\,\mathbf{u}^p_{e,f}=\mathbf{RU} \tag{5}$$

$$\mathbf{x}^p(r,s)=\sum_{e=i-p_1}^{i}\sum_{f=j-p_2}^{j}R_{e,f}(r,s)\mathbf{x}^p_{e,f}=\mathbf{RX} \tag{6}$$

The strain-displacement matrix $\mathbf{B}$ can be constructed from the following fundamental equations

$$\boldsymbol{\varepsilon}=\mathbf{Du}\quad\rightarrow\quad\boldsymbol{\varepsilon}=\mathbf{BU} \tag{7}$$

where $\mathbf{D}$ is the differential operation matrix. Following a standard approach for the derivation of the finite elements formulation, the matrix of coefficient can easily be obtained. For example, by implementing the virtual displacement method with existence of body forces $\mathbf{b}$ and traction forces $\mathbf{t}$ we can write

$$\int_{V^p}\delta\boldsymbol{\varepsilon}^T\boldsymbol{\sigma}\,dV-\int_{V^p}\delta\mathbf{u}^T\mathbf{b}\,dV-\int_{\Gamma^p}\delta\mathbf{u}^T\mathbf{t}\,d\Gamma=0\,, \tag{8}$$

where V^p and Γ^p are the volume and the boundary of patch p.

Now, by substituting $\delta\boldsymbol{\varepsilon}=\mathbf{B}\delta\mathbf{U}$ from (7) and the constitutive equation $\boldsymbol{\sigma}=\mathbf{C}\boldsymbol{\varepsilon}$, in (8) and by dropping the coefficient of $\delta\mathbf{U}^T$, the matrix of coefficients can be obtained as

$$\mathbf{K}^p=\int_{V^p}\mathbf{B}^T\mathbf{CB}\,dV \tag{9}$$

As it is noted, in the equations above, all of the variables are written in terms of the parameters r and s which is similar to mapping in the standard finite element method where the base or unit elements are used. However, calculation of the partial differentials is somehow different and needs special

care. With some simple calculus the following relations can be derived:

$$\frac{\partial u}{\partial x}=\frac{\frac{\partial u}{\partial r}\frac{\partial y}{\partial s}-\frac{\partial u}{\partial s}\frac{\partial y}{\partial r}}{\frac{\partial x}{\partial r}\frac{\partial y}{\partial s}-\frac{\partial x}{\partial s}\frac{\partial y}{\partial r}},\quad \frac{\partial u}{\partial y}=\frac{-\frac{\partial u}{\partial r}\frac{\partial x}{\partial s}-\frac{\partial u}{\partial s}\frac{\partial x}{\partial r}}{\frac{\partial x}{\partial r}\frac{\partial y}{\partial s}-\frac{\partial x}{\partial s}\frac{\partial y}{\partial r}} \tag{10}$$

Similar formulas can be obtained for unknown variable v. In this research the standard Gauss quadrature over each knot space is used for numerical integration. The proper number of gauss points depends on the order of the NURBS basis functions.

3 Topology optimization problem

The problem at hand is defined as finding the stiffest possible structure when a certain amount of material is given. A structure with maximum global stiffness provides a minimum for the external work with the real displacement field or minimum mean compliance. Since, minimization of mean compliance is equivalent to the maximization of the total potential energy, the topology optimization problem can be constructed as below (Hassani and Hinton 1999; Bendsøe and Sigmund 2003)

$$\begin{array}{ll}\max & \min\ \Pi(\mathbf{u})\\ \textit{subject to} & \Omega_s \le \bar{\Omega}_s\\ \textit{and} & \textit{design restrictions}\end{array} \tag{11}$$

where $\mathbf{u}$ is displacement field, Π is total potential energy and $\bar{\Omega}_s$ is the amount of material available. Ω_s is the volume of solid material in each design. One should note that minimization of $\Pi(\mathbf{u})$ in (11) is equivalent to satisfying the state equations or equilibrium. $\Pi(\mathbf{u})$ can be written as follows

$$\Pi(\mathbf{u})=\frac{1}{2}\int_\Omega \boldsymbol{\varepsilon}^T(\mathbf{u})\mathbf{C}\boldsymbol{\varepsilon}(\mathbf{u})\,d\Omega-\int_\Omega \mathbf{u}^T\mathbf{f}\,d\Omega-\int_\Gamma \mathbf{u}^T\mathbf{t}\,d\Gamma \tag{12}$$

In structural topology optimization, the problem is how to distribute the material in order to minimize the objective function. In other words, the goal can be thought of as determination of the optimal spatial material distribution and can be described as a density function $\phi(\mathbf{x})$ for every point of the design domain $\mathbf{x}$.

$$\phi(\mathbf{x})=\begin{cases}1 & \textit{if}\quad \mathbf{x}\in\Omega_s\\ 0 & \textit{if}\quad \mathbf{x}\in\Omega\backslash\Omega_s\end{cases} \tag{13}$$

The above material distribution function can be approximated by the NURBS basis functions over a patch.

$$\phi^p(\mathbf{r})=\sum_{i=0}^{n_1}\sum_{j=0}^{n_2}R_{i,j}(\mathbf{r})\Phi_{i,j}^p \tag{14}$$

where $\Phi_{i,j}^p$ are control points of the NURBS surface in patch p and can be assumed as design variables of the optimization problem. It is noted that the same basis functions are used for approximation of geometry, displacements and the density function.

Inspired by the SIMP method, in order to prevent the porous area, the density function is penalized for evaluating the artificial density and elasticity matrix. Therefore,

$$\begin{aligned}\rho(\mathbf{x})&=\varphi(\mathbf{x})\rho^0\\ \mathbf{C}(\mathbf{x})&=\varphi(\mathbf{x})^\mu\mathbf{C}^0\end{aligned} \tag{15}$$

where ρ^0 and $\mathbf{C}^0$ are the density and elasticity matrix of solid material, respectively. The discretized optimization problem can be written as below:

$$\begin{array}{lll}\max\limits_{\Phi_{i,j}} & \min\limits_{i=1,\ldots,n_1,\ j=1,\ldots,n_2}\ \Pi(\mathbf{u}) & \\ \textit{subject to} & \Phi_{i,j}-1\le 0 & i=1,\ldots,n_1,\ j=1,\ldots,n_2\\ & -\Phi_{i,j}\le 0 & i=1,\ldots,n_1,\ j=1,\ldots,n_2\\ \textit{and} & \Omega_s\le\bar{\Omega}_s & \end{array} \tag{16}$$

The Lagrangian function ℓ of the optimization problem can be constructed by using the Lagrange multipliers

$$\begin{aligned}\ell=\Pi(\mathbf{u})&-\Lambda\left(\Omega_s-\bar{\Omega}_s\right)-\sum_{i,j=1}^{n\times m=N}\lambda_1\left(\Phi_{i,j}-1\right)\\ &-\sum_{i,j=1}^{n\times m=N}\lambda_2\left(-\Phi_{i,j}\right)\end{aligned} \tag{17}$$

where Λ, λ_1 and λ_2 are the volume, upper and lower bound Lagrange multipliers, respectively, which are positive according to the Kuhn–Tucker conditions (Hassani and Hinton 1999). The stationary condition with respect to the design variables $\Phi_{i,j}$ can be obtained as follows

$$\frac{\partial\Pi(\mathbf{u})}{\partial\Phi_{i,j}}-\Lambda\frac{\partial\Omega_s}{\partial\Phi_{i,j}}-\lambda_1+\lambda_2=0 \tag{18}$$

By manipulating the above equation it can be written as

$$E_{i,j}=1+\lambda_1/\Lambda\frac{\partial\Omega_s}{\partial\Phi_{i,j}}-\lambda_2/\Lambda\frac{\partial\Omega_s}{\partial\Phi_{i,j}} \tag{19}$$

where

$$E_{i,j} = \frac{\frac{1}{2}\int_{\Omega} \boldsymbol{\varepsilon}^T \frac{\partial \mathbf{C}}{\partial \Phi_{i,j}} \boldsymbol{\varepsilon}\, d\Omega}{\Lambda \int_{\Omega} \frac{\partial \phi}{\partial \Phi_{i,j}}\, d\Omega} \tag{20}$$

It can be assumed that in iteration k, the design variable $\Phi_{i,j}$ has been decreased in order to move toward optimum point. Therefore, $\Phi_{i,j} < 1$ and the upper side limit is not active,

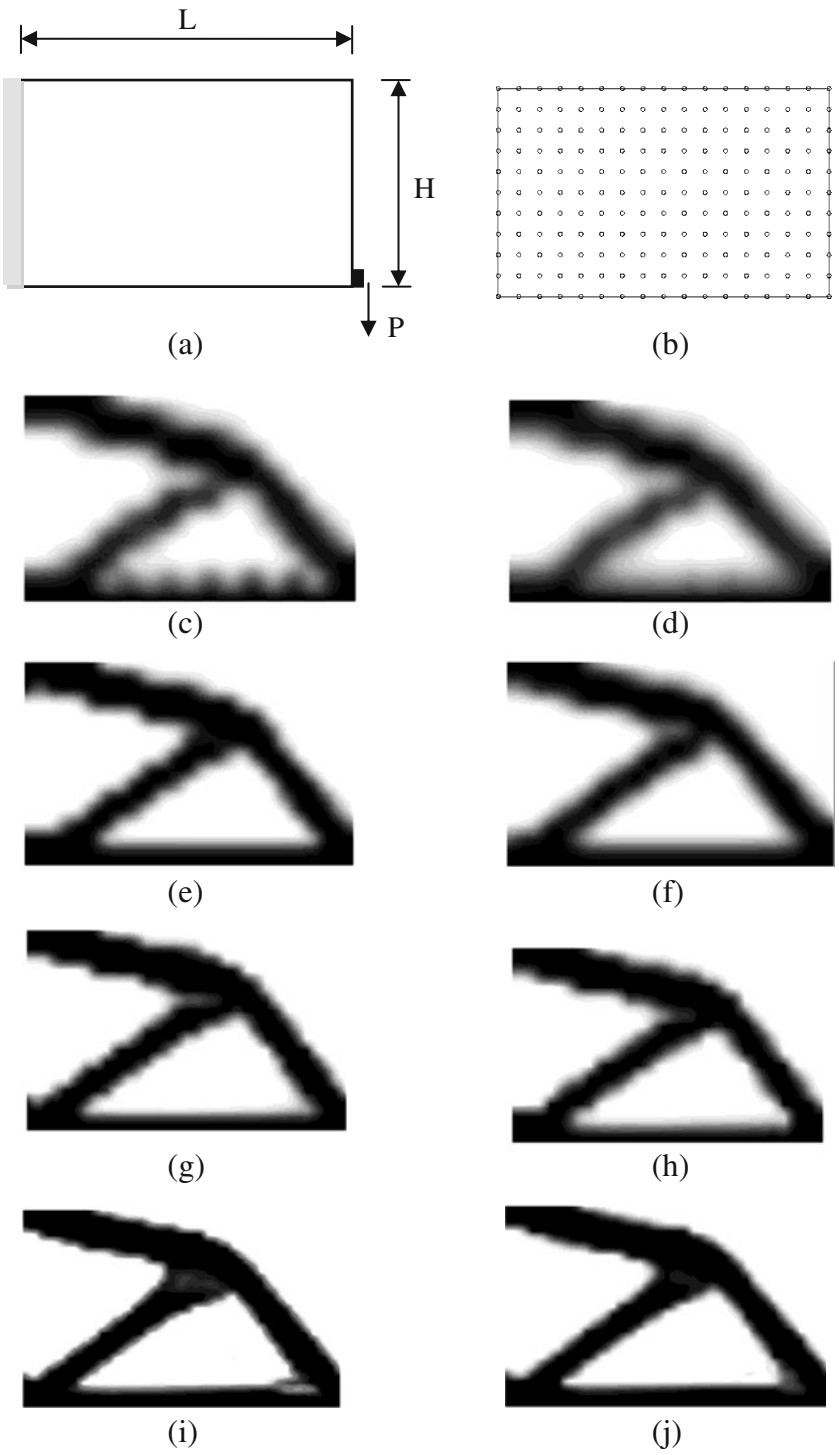

Fig. 1 Short cantilever beam: **a** problem definition, **b** Control net with $17 \times 11 = 187$ points, **c**, **d** optimum topologies by using 187, **e**, **f** 400, **g**, **h** 693 and **i**, **j** 1617 control points for degree of NURBS' basis functions equal to 2 and 3, respectively

which yields $\lambda_1 = 0$. Since $\Lambda \int_\Omega \frac{\partial \varphi}{\partial \Phi_{i,j}} \, d\Omega$ is a positive real number and $\lambda_2 \geq 0$, from (19) it follows that $E^k_{i,j} \leq 1$. On the other hand, increasing $\Phi_{i,j}$, results $E^k_{i,j} \geq 1$. Inspired by this argument, $E^k_{i,j}$ is calculated and compared with unity. If $E^k_{i,j} < 1$ then $\Phi_{i,j}$ is decreased by the move limit ξ and vice versa. Based on this conclusion and considering the side limits, Bendsøe and Sigmund (2003) have suggested the following resizing scheme.

$$\Phi^{k+1}_{i,j} = \begin{cases} \max\left\{(1-\xi)\Phi^k_{i,j}, \Phi^{\min}_{i,j}\right\} & \text{if } \Phi^k_{i,j}\left(E^k_{i,j}\right)^\eta \leq \max\left\{(1-\xi)\Phi^k_{i,j}, \Phi^{\min}_{i,j}\right\} \\ \min\left\{(1+\xi)\Phi^k_{i,j}, \Phi^{\max}_{i,j}\right\} & \text{if } \min\left\{(1+\xi)\Phi^k_{i,j}, \Phi^{\max}_{i,j}\right\} \leq \Phi^k_{i,j}\left(E^k_{i,j}\right)^\eta \\ \Phi^k_{i,j}\left(E^k_{i,j}\right)^\eta & \text{otherwise} \end{cases} \tag{21}$$

where η is a damping factor and superscript k denotes the iteration number. It is important to note that $E_{i,j}$ depends on the current value of Λ_k which needs to be adjusted in an inner iteration loop. For this purpose the bisection method can be employed (Suzuki and Kikuchi 1991).

4 Numerical examples

To demonstrate the performance of the method four examples of isotropic plane elasticity problems are presented in this section. In all examples the modulus of elasticity and the Poisson's ratio are considered as 1,500 kgf/cm^2 and 0.3, respectively. Also, the exponent $\mu = 3$ is used for penalizing the density function. In all of the following examples dimensions are considered as $L = 8$ cm and $H = 5$ cm except example five where these are set $L = 12$ cm and $H = 2$ cm. Also, the point load magnitude is assumed to be $P = 100$ kgf.

Example 1 A cantilever beam subject to a point load at the bottom corner is considered as shown in Fig. 1a. In this example, the effect of different number of discretizing control points is studied. In all of the discretizations equally spaced open knot vectors are used for each direction. The considered knot vectors are given in Table 1. The volume fraction in all cases is taken as $\Omega_s/\Omega_{total} = 40\%$.

In the first experience only one patch including $11 \times 17 = 187$ control points, as shown in Fig. 1b, was considered. The optimum topology, when the degrees of the NURBS' basis functions are assumed to be $p_1 = p_2 = 2$ in both directions, is illustrated in Fig. 1c. The obtained layout for $p_1 = p_2 = 3$ is illustrated in Fig. 1d. In the second experience, again, only one patch with 400 control points was employed. The obtained optimum layouts are shown in Fig. 1e and f for $p_1 = p_2 = 2$ and $p_1 = p_2 = 3$, respectively.

As the third experience, to study the effect of having more patches and a finer discretization, 40 patches with 693 control points were adopted. The optimum layouts for this case are shown in Fig. 1g and h for the degrees of basis functions equal to 2 and 3, respectively. In the last experience, a net of control points with 96 patches and 1,617 control points were used and the obtained layouts are depicted in Fig. 1i and j for the NURBS basis functions of degrees 2 and 3 in both directions, respectively.

Table 1 Considered knot vectors for each patch

No. of control points	No. of patches	The employed equally spaced knot vectors
187	1	$\mathbf{r} = \{0,0,0,0.066,...,0.933,1,1,1\}$, $\mathbf{s} = \{0,0,0,0.111,...,0.888,1,1,1\}$ *for* $p_1 = p_2 = 2$
		$\mathbf{r} = \{0,0,0,0.071,...,0.929,1,1,1\}$, $\mathbf{s} = \{0,0,0,0.125,...,0.875,1,1,1\}$ *for* $p_1 = p_2 = 3$
400	1	$\mathbf{r} = \{0,0,0,0.044,...,0.957,1,1,1\}$, $\mathbf{s} = \{0,0,0,0.071,...,0.928,1,1,1\}$ *for* $p_1 = p_2 = 2$
		$\mathbf{r} = \{0,0,0,0,0.045,...,0.955,1,1,1,1\}$, $\mathbf{s} = \{0,0,0,0,0.077,...,0.923,1,1,1,1\}$ *for* $p_1 = p_2 = 3$
693	40	$\mathbf{r} = \{0,0,0,0.333,0.666,1,1,1\}$, $\mathbf{s} = \{0,0,0,0.333,0.666,1,1,1\}$ *for* $p_1 = p_2 = 2$
		$\mathbf{r} = \{0,0,0,0,0.5,1,1,1,1\}$, $\mathbf{s} = \{0,0,0,0,0.5,1,1,1,1\}$ *for* $p_1 = p_2 = 3$
1,617	96	$\mathbf{r} = \{0,0,0,0.333,0.666,1,1,1\}$, $\mathbf{s} = \{0,0,0,0.333,0.666,1,1,1\}$ *for* $p_1 = p_2 = 2$
		$\mathbf{r} = \{0,0,0,0,0.5,1,1,1,1\}$, $\mathbf{s} = \{0,0,0,0,0.5,1,1,1,1\}$ *for* $p_1 = p_2 = 3$

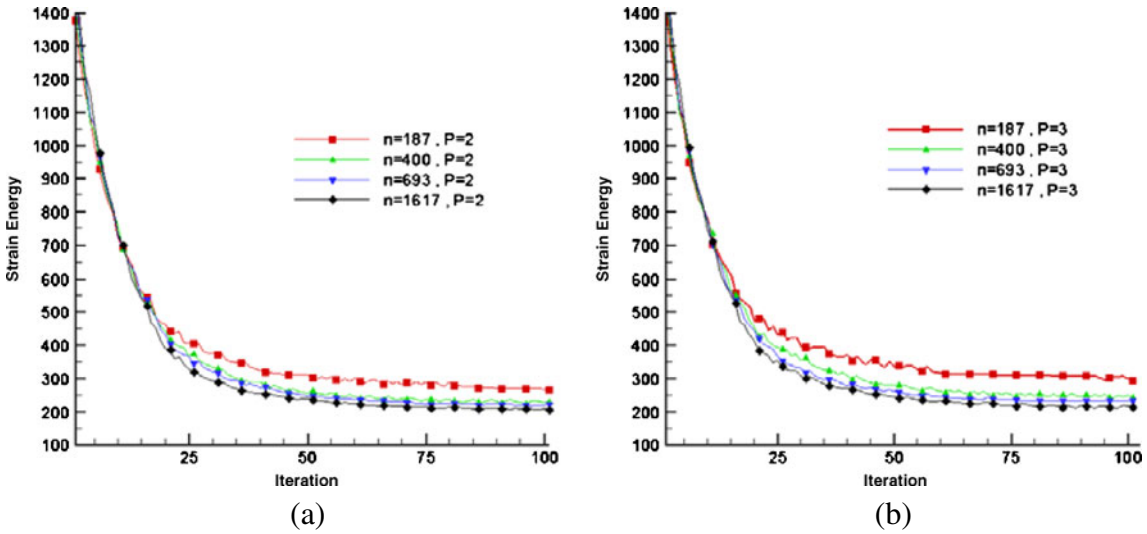

Fig. 2 Iteration history of short cantilever beam: **a** $p_1 = p_2 = 2$ and **b** $p_1 = p_2 = 3$

As it is observed, in all of the experiences, by increasing the degree of the NURBS' basis functions smoother boundaries are resulted. Also, by increasing the number of control points, either by using extra patches or with only one patch, layouts with less intermediate material densities, i.e. gray areas, are obtained. A very important feature, in contrast with the finite element approach that will be further elaborated in the following, is that in all the experiences, the resulted topology is the same and independent of the polynomial degrees as well as number of discretization points.

The histories of variations of the objective functions for $p = 2$ and $p = 3$ are illustrated in Fig. 2a and b, respectively. As it is observed, by increasing the number of control points better values for the objective function, i.e. strain energy, are obtained.

For the sake of comparison of the performances, this problem is here solved again by using the finite elements together with the SIMP method. In the first try a mesh of 384 quadratic eight-node finite elements with 1,233 nodes is employed and the volume fraction and the penalty exponent were taken as before. The obtained topology is depicted in Fig. 3a. In the next experience, a mesh of 1,000 quadratic finite elements with 3,131 nodes, and other parameters the same as before, were used and the obtained optimal layout is shown in Fig. 3b. As it is observed, the obtained topologies are different which was expected as a very well known instability problem. It should be noted that when this problem is solved with bilinear four-node elements, the instability of creation of checker-boarding patterns are occurred that is shown in Fig. 3c. The interested reader is encouraged to consult Hassani and Hinton (1999), Bendsøe and Sigmund (2003) and Sigmund (1998) for more information. Amongst different methods for removing these instabilities, when the noise cleaning technique, proposed by Bendsøe and Sigmund (2003), is employed, the obtained optimum layouts with the formerly mentioned finite element meshes are shown in Fig. 4a–c. It is noticed that the obtained topology is the same for all finite element meshes which is also the same as all of the four different isogeometrical solutions as depicted in Fig. 1.

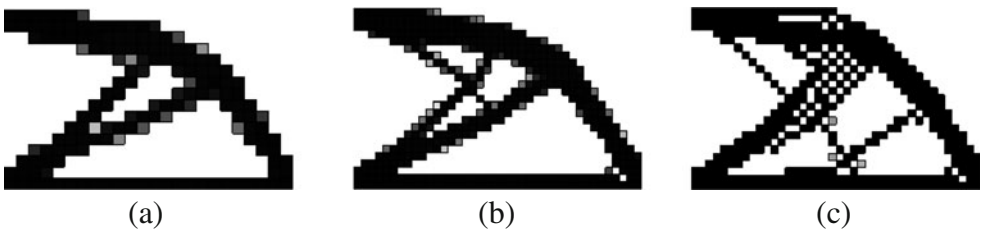

Fig. 3 Optimum topology of short cantilever beam with **a** 384 eight-node, **b** 1,000 eight-node **c** 1,000 four-node finite elements

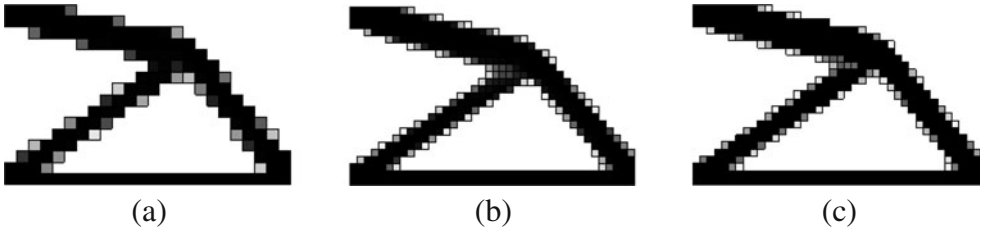

Fig. 4 Optimum topology of short cantilever beam by using noise cleaning techniques with **a** 384 eight-node, **b** 1,000 eight-node and **c** 1,000 four-node finite elements

Example 2 The geometry, loading and boundary conditions are illustrated in Fig. 5. In this example the ability of the proposed method in capturing the optimum topology and the effect of the number of control points is studied. For this purpose, a couple of control nets with 400 and 1,617 points are used for discretizing the design domain as well as the material density function. The degree of the NURBS' basis functions is assumed $p = 3$. The resulted layouts are depicted in Fig. 6a and b. Three dimensional graph of the density functions are shown in Fig. 6c and d. As it is observed, the number of control points has not changed the topology. The optimal design form Sigmund's 99 line MATLAB code (Sigmund 2001) is illustrated in Fig. 7. It should be noted that in this code noise cleaning technique is implemented in order to prevent checker-boarding and mesh dependency instabilities. It can be seen that the obtained topologies in both methods are identical.

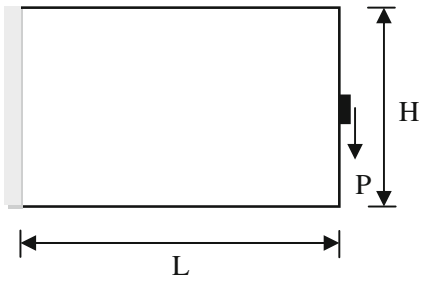

Fig. 5 Problem definition of Example 2

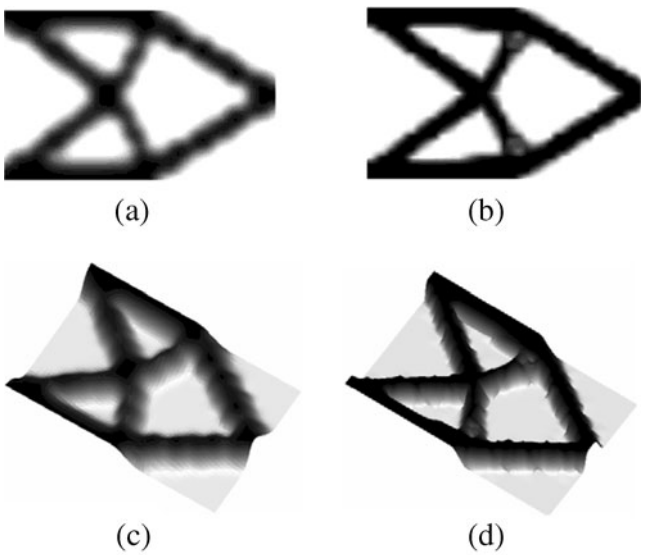

Fig. 6 **a**, **c** Optimum layout by using 400, **b**, **d** by using 1617 control points

Example 3 The value of the specified material volume in the design domain can affect the optimal topology. To demonstrate this, a short beam problem is solved with three different volume fractions 50%, 30% and 20%. The design domain, supports of beam and loading are shown in Fig. 8. In this example, 96 patches with 1,617 control points are used for discretizing the design domain and the degree of NURBS' basis functions is 3. The employed knot vectors are the same as Example 1 (Fig. 9).

Example 4 In this example a cantilever beam with a fixed hole is considered. The problem description and the arrangement of the control points in two different patches are given in Fig. 10. The considered design domain is more complicated than previous examples and is here created by 804 control point. As it is shown in Fig. 10, nine

Fig. 7 Optimum layout by SIMP and FEM (Sigmund 2001)

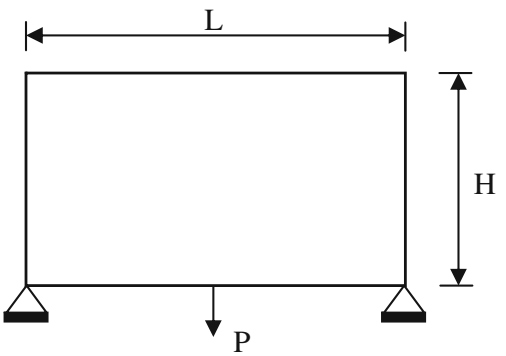

Fig. 8 Problem definition of Example 3

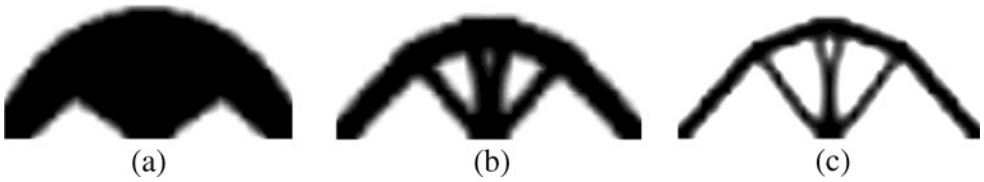

Fig. 9 Optimum layout by using **a** $\Omega_s/\Omega_{total} = 50\%$ **b** $\Omega_s/\Omega_{total} = 30\%$ **c** $\Omega_s/\Omega_{total} = 20\%$

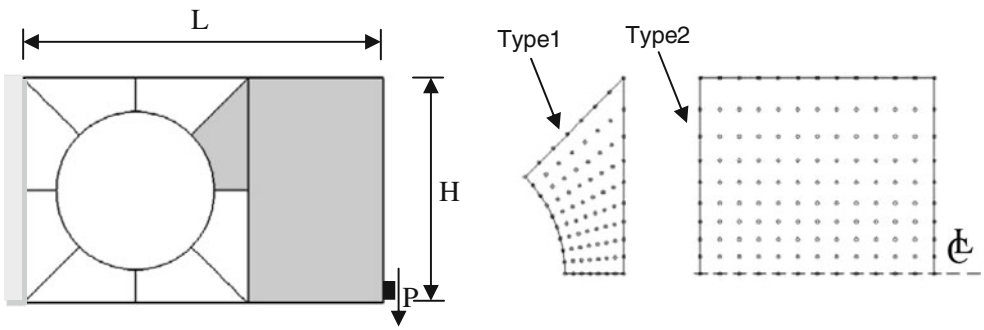

Fig. 10 Problem definition and control points arrangement for two different patches

NURBS patches of two different types are used for discretization. The volume fraction is taken as 40%. Equally spaced knot vectors for two types of patches are given in Table 2. The obtained topology is illustrated in Fig. 11. One should note that solving this problem with the FEM requires an unstructured mesh with a considerable large number of finite elements.

Example 5 Topology optimization of the MBB beam is here considered as the final example. The design domain and boundary conditions are shown in Fig. 12. In order to discretize the design domain 95 patches with 1,617 control points are employed. The degree of the NURBS' basis functions is considered to be 3. The volume fraction is taken as 40%. Equally spaced knot vectors are defined as $\mathbf{r} = \{0, 0, 0, 0, 0.5, 1, 1, 1, 1\}$, $\mathbf{s} = \{0, 0, 0, 0, 0.5, 1, 1, 1, 1\}$. The obtained layout by employing the proposed method, without using any extra noise cleaning or image processing technique, is illustrated in Fig. 13a. For the sake of comparison, the result generated by using the SIMP material model together with the finite elements, as reported in Hassani and Hinton (1999),

Table 2 Considered knot vectors for each patch

Patch type	Patch order p	Equally spaced knot vectors
1	2	$\mathbf{r} = \{0, 0, 0, 0.166, ..., 0.833, 1, 1, 1\}$, $\mathbf{s} = \{0, 0, 0, 0.125, ..., 0.875, 1, 1, 1\}$
1	3	$\mathbf{r} = \{0, 0, 0, 0, 0.2, ..., 0.8, 1, 1, 1, 1\}$, $\mathbf{s} = \{0, 0, 0, 0, 0.143, ..., 0.857, 1, 1, 1, 1\}$
2	2	$\mathbf{r} = \{0, 0, 0, 0.0909, ..., 0.909, 1, 1, 1\}$, $\mathbf{s} = \{0, 0, 0, 0.0588, ..., 0.9408, 1, 1, 1\}$
2	3	$\mathbf{r} = \{0, 0, 0, 0, 0.1, ..., 0.9, 1, 1, 1, 1\}$, $\mathbf{s} = \{0, 0, 0, 0, 0.0625, ..., 0.9375, 1, 1, 1, 1\}$

Fig. 11 Optimum topology of Example 4 **a** by using $p_1 = p_2 = 2$ **b** by using $p_1 = p_2 = 3$

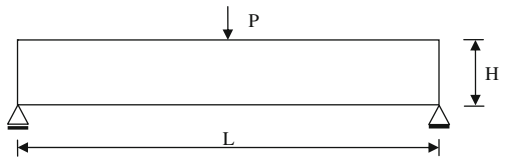

Fig. 12 Problem definition of Example 5

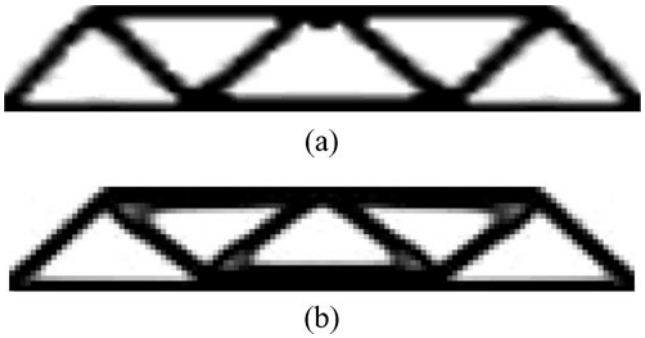

Fig. 13 Optimum layouts by using **a** the current approach and **b** SIMP and FEM (Sigmund 2001)

Bendsøe and Sigmund (2003) and Sigmund (1998, 2001), is also shown in Fig. 13b. As it is observed the obtained topologies are basically the same. However, it is noticed that the gray areas at some of the corners of the diagonal members do not exist in the result by the proposed method.

5 Conclusion

In this paper, a new approach is presented for structural topology optimization where the material distribution function is approximated by using NURBS' basis functions over the whole domain. Also, the IA method is used for analysis of plane elasticity problems. When the finite element method is employed for the several analyses involved in the topology optimization problem, the design variables, no matter what material model is used, are assumed as constant variables inside each finite element. Hence, the obtained layouts are not independent from the employed finite element mesh. By using the isogeometrical analysis method, the control points of the material distribution function, which can be imagined as a surface in plane elasticity, are taken as the design variable of the optimization problem. Therefore, a smooth continuous function over the whole design domain is constructed which removes the problems of mesh dependency. Although more research needs to be carried out, these early results are supporting this idea and are indicating that the property of smooth distribution of material is the reason for independency of the obtained layouts from the domain discretization. In other words, according to our experience, even with a coarse net of control points, one ends up with the correct topology that is always checkerboard free, which is not the case when the finite element method is used.

References

Allaire G, Jouve F, Toader AM (2004) Structural optimization using sensitivity analysis and a level-set method. J Comput Phys 194:363–393

Bazilevs Y, Beirao Da Veiga L, Cottrell J, Hughes TJR, Sangalli G (2006a) Isogeometric analysis: approximation, stability and error estimates for h-refined meshes. Math Models Methods Appl Sci 16:1031–1090

Bazilevs Y, Calo VM, Zhang Y, Hughes TJR (2006b) Isogeometric fluid structure interaction analysis with applications to arterial blood flow. Comput Methods Appl Mech Eng 38:310–322

Bazilevs Y, Calo V, Cottrell J, Hughes TJR, Reali A, Scovazzi G (2007) Variational multiscale residual-based turbulence modeling for large eddy simulation of incompressible flows. Comput Methods Appl Mech Eng 197:173–201

Belytschko T, Xiao SP, Parimi C (2003) Topology optimization with implicit functions and regularization. Int J Numer Methods Eng 57:1177–1196

Bendsøe MP, Kikuchi N (1988) Generating optimal topologies in structural design using homogenization method. Comput Methods Appl Mech Eng 71:197–224

Bendsøe MP, Sigmund O (2003) Topology optimization. Theory, methods and applications. Springer, Germany

Cottrell JA, Reali A, Bazilevs Y, Hughes TJR (2006) Isogeometric analysis of structural vibrations. Comput Methods Appl Mech Eng 195:5257–5296

Fanjoy D, Crossley W (2000) Using a genetic algorithm to design beam corss-sectional topology for bending, torsion, and combined loading. In: Structural dynamics and material conference and exhibit. AIAA, Atlanta, GA, pp 1–9

Fleury C (1989) CONLIN: an efficient dual optimizer based on convex approximation concepts. Struct Multidisc Optim 1:81–89

Hassani B, Hinton E (1999) Homogenization and structural topology optimization: theory, practice and software. Springer, London

Hassani B, Khanzadi M, Tavakkoli SM, Moghaddam NZ (2009a) Isogeometric shape optimization of three dimensional problems. In: 8th world congress on structural and multidisciplinary optimization, 1–5 June, Lisbon, Portugal

Hassani B, Moghaddam NZ, Tavakkoli SM (2009b) Isogeometrical solution of Laplace equation. Asian J Civil Eng 10(5):572–592

Hughes TJR, Cottrell JA, Bazilevs Y (2005) Isogeometric analysis: CAD, finite elements, NURBS, exact geometry and mesh refinement. Comput Methods Appl Mech Eng 194:4135–4195

Jakiela MJ, Chapman C, Duda J, Adewuya A, Saitou K (2000) Continuum structural topology design with genetic algorithms. Comput Methods Appl Mech Eng 186:339–356

Kane C, Schoenauer M (1996) Topological optimum design using genetic algorithms. Control Cybernatics (Special Issue on Optimum Design) 25(5):1059–1088

Kaveh A, Hassani B, Shojaee S, Tavakkoli SM (2008) Structural topology optimization using ant colony methodology. Eng Struct 30(9):2559–2565

Michell AGM (1904) The limits of economy of material in frame structures. Philos Mag 8:305–316

Piegl L, Tiller W (1997) The NURBS book. Springer, New York

Rozvany GIN (1989) Structural design via optimality criteria. Kluwer, Dordrecht

Rozvany GIN (2010) A critical review of established methods of structural topology optimization. Struct Multidisc Optim 37:217–237

Rozvany GIN, Zhou M, Birker T (1992) Generalized shape optimization without homogenization. Struct Optim 4:250–254

Schmit LA, Farsi B (1974) Some approximation concepts for structural synthesis. AIAA J 12(5):692–699

Schmit LA, Miura H (1976) Approximation concepts for efficient structural synthesis. NASA, Washington, DC, CR-2552

Sethian J, Wiegmann A (2000) Structural boundary design via level set and immersed interface methods. J Comput Phys 163:489–528

Sigmund O (1998) Numerical instabilities in topology optimization: a survey on procedure dealing with checkerboards, mesh-dependencies and local minima. Review Article Structural Optimization 16:68–75

Sigmund O (2001) A 99 line topology optimization code written in MATLAB. Struct Multidisc Optim 21:120–127

Suzuki K, Kikuchi N (1991) A homogenization method for shape and topology optimization. Comput Methods Appl Mech Eng 93:291–318

Svanberg K (1987) The method of moving asymptotes—a new method for structural optimization. Int J Numer Methods Eng 24:359–373

Vanderplaats GN, Salajegheh E (1989) A new approximation method for stress constraints in structural synthesis. AIAA J 27(3):352–358

Wang MY, Wang X, Guo D (2003) A level-set method for structural topology optimization. Comput Methods Appl Mech Eng 192:227–246

Xie YM, Steven GP (1993) A simple evolutionary procedure for structural optimization. Comput Struct 885–896

Zhou M, Rozvany GIN (1991) The COC algorithm, part I: cross section optimization or sizing. Comput Methods Appl Mech Eng 89:281–308

Zhou JX, Zou W (2008) Meshless approximation combined with implicit topology description for optimization of continua. Struct Multidisc Optim 36:347–353